

The heterotrophic bacterial response during the Southern Ocean Iron Experiment (SOFeX)

Jacques L. Oliver¹

Virginia Institute of Marine Science, College of William and Mary, Gloucester Point, Virginia 23062

Richard T. Barber

Nicholas School of the Environment and Earth Sciences, Duke University, Beaufort, North Carolina 28516

Walker O. Smith, Jr., and Hugh W. Ducklow

Virginia Institute of Marine Science, College of William and Mary, Gloucester Point, Virginia 23062

Abstract

We studied heterotrophic bacterial dynamics as part of the Southern Ocean Iron Experiment (SOFeX), January–February 2002. Two phytoplankton blooms were monitored following infusions with iron sulfate (FeSO_4). The first bloom was initiated north of the Antarctic Polar Front Zone (APFZ) in silica-poor waters (North Patch) and was observed sporadically over 42 d, whereas the second was south of the APFZ in silica-rich waters (South Patch) and was continuously observed for 30 d. In both experiments, iron additions resulted in increased chlorophyll *a* (Chl *a*), particulate organic matter (POC + PN), and a drawdown of inorganic nutrients. Heterotrophic bacteria responded by increasing their abundance (110% and 60% increases in bacterial abundance in the North and South Patch, respectively, relative to nonenriched waters). Thymidine (TdR) and leucine (Leu) incorporation rates in the North Patch increased by 400% and 120%, respectively, with more modest increases in the South Patch (80% and 70%, respectively). In the South Patch, bacterial production (BP) was significantly correlated with net particulate primary production (PP) and Chl *a*. Bacterial abundance was also significantly correlated with Chl *a*. Net bacterial accumulation rate in the South Patch was 0.02 d^{-1} over 17 d, excluding physical dilution by mixing with water outside the South Patch. The evidence suggests that bacterial growth during Southern Ocean Iron Experiment (SOFeX) was limited by labile carbon rather than by iron. Despite the close association of BP to PP, BP remained a small fraction of PP (<10%).

After more than a decade of testing the iron hypothesis (Martin et al. 1994), it is clear that iron plays a central role in regulating phytoplankton production in the ocean, particularly in high-nutrient, low-chlorophyll (HNLC) regions. Repeated mesoscale open-ocean iron experiments have improved our overall understanding of ocean biogeochemistry. Numerous geochemical (Bakker et al. 2001) and food-web effects (Landry et al. 2000) were observed following iron enrichment. These experiments have provided insights into paleobiogeochemistry (Bidigare et al. 1999) and even sparked controversy over the potential role of iron in ame-

liorating long-term global climate change (Chisholm et al. 2001).

Iron-enrichment experiments also demonstrated the stimulation of one component of natural carbon storage in the ocean: the biological pump (Ducklow et al. 2001b). In HNLC regions like the Southern Ocean, dissolved iron is the primary rate-limiting factor of the first component of the biological pump, primary production. Iron enrichments have demonstrated priming of the biological pump but have yet to unequivocally demonstrate carbon export to the ocean interior (Ducklow et al. 2003). Heterotrophic bacteria may influence the efficiency of carbon export through the remineralization of organic material (either particulate organic matter [POM] or dissolved organic matter [DOM]), thus retarding its export from the surface ocean. During the creation of bacterial biomass, bacterial respiration returns organic matter back to the inorganic phase. This process counteracts the autotrophic carbon fixation process and serves as a balance to organic carbon production (particulate organic [POC] and dissolved organic carbon [DOC]).

Understanding growth constraints on heterotrophic bacteria can provide insights into the degree to which they can mediate organic carbon fluxes in the ocean. Iron limitation (Pakulski et al. 1996), DOM limitation (Hall and Safi 2001), and colimitation by iron and DOM together (Church et al. 2000) have been suggested for different areas of the Southern Ocean. Evidence for bacterial growth limitation by iron

¹ Corresponding author (jloiver@vims.edu).

Acknowledgments

We thank M. Landry and S. Brown (Univ. Hawaii) for use of microzooplankton grazing data, M. Altabet (Univ. Massachusetts) for use of POM data, and J. A. Hall (N.I.W.A. New Zealand) for contributing reagents for BP measurements. We express our gratitude to the captain and crew of RV *Melville* and RV *Revelle*, respectively, for their operational support and the SOFeX group for their organizational support. L. Delizo and E. Bailey provided assistance in collecting bacterial samples and H. Quinby assisted in flow cytometry. We are also grateful to A. Hiltling, M. Hiscock, A. Aprill, and V. Lance for primary production measurements.

This work is supported by NSF OPP-000329 to H.W.D and W.O.S., Jr., DE-FG02-01 ER63082 to W.O.S., Jr., and NSF OCE-9911441 to R.T.B.

This is JGOFS contribution 1027.

in other HNLC regions is sparse, with DOM limitation being more widespread (Kirchman et al. 2000).

The objective of our study was twofold. The first objective was to measure the response of heterotrophic bacteria to iron enrichment and to determine whether the response was directly or indirectly stimulated by iron. We hypothesized that bacterial production would increase as a direct consequence of increased DOC production from iron-stimulated phytoplankton rather than as a direct response to iron. Furthermore, we predicted that, while bacterial production would increase, bacterial biomass would not (e.g., Hall and Safi 2001). The second objective was to understand the bacterial response as part of a broader plankton and biogeochemical response to iron enrichment. Overall, we seek to understand the controlling factor(s) of heterotrophic bacterial activity and the degree and timescales on which this activity modifies biological pump efficiency during phytoplankton blooms in the Southern Ocean.

Materials and methods

Study site—Two iron enrichment experiments were performed in the HNLC Pacific Ocean sector of the Southern Ocean during the late austral summer 2002 (January–February) (Coale et al. 2004). The first experiment took place north of the Antarctic Polar Front Zone (APFZ) in low-iron, low-silica, high-NO₃ waters (<0.1 nmol Fe L⁻¹, 3 μmol Si L⁻¹, 22 N μmol L⁻¹, respectively) near 56°S, 172°W and was designated the North Patch. The second took place south of the APFZ in low-iron, high-silica, high-NO₃ waters (0.1 nmol Fe L⁻¹, 60–64 μmol Si L⁻¹, 28 N μmol L⁻¹, respectively) near 66°S, 171°W and was designated the South Patch. Water temperatures in the North and South Patches were 7°C and -1°C, respectively. All bacterial, primary production, and POM measurements reported herein were made aboard the RV *Melville*. Initial hydrographic measurements were made aboard from the RV *Revelle* during surveys prior to the iron additions.

Heterotrophic bacteria—Water was collected with Niskin bottles from depths of 5, 10, 20, 30, 40, and 50 m or from transects across the South Patch at depths of 10 and 50 or 60 m. Bacterial abundance was determined by flow cytometry (FCM) following the methods of Troussellier et al. (1999). Flow cytometry samples were fixed with 0.2-μm-filtered formalin (1% final concentration) and stored at -80°C until analysis. Triplicate 1-ml subsamples were stained with Syto13 (Molecular Probes) and counted on a Beckman-Coulter Epics Altra flow cytometer equipped with an Enterprise II laser at 488 nm. Count calibration was performed by adding 1.0-μm beads (Molecular Probes, Fluospheres) at a concentration of 5 × 10⁴ beads ml⁻¹ to each subsample. A minimum of 10,000 cells was counted from each subsample. Intrasample variation was less than 1%. High DNA- (HDNA) and low DNA-containing (LDNA) cells were differentiated by fluorescence (Gasol and Moran 1999).

Bacterial production (BP) was estimated via tritiated thymidine (³H-TdR) and leucine (³H-Leu) incorporation using the microcentrifuge method described by Smith and Azam

(1992). Briefly, separate incubations for ³H-TdR and ³H-Leu incorporation were carried out in triplicate 2-ml microcentrifuge tubes containing 20 nmol L⁻¹ ³H-TdR (specific activity: 88.7 Ci mmol⁻¹) or 20 nmol L⁻¹ ³H-Leu (specific activity: 172 Ci mmol⁻¹). Killed controls contained the same concentrations of ³H-TdR and ³H-Leu but with 100 μl 100% trichloroacetic acid (TCA). Incubation times ranged between 8 and 14 h, depending on the ambient water temperature (Church et al. 2000). All incubations were carried out in the dark at ambient temperature in a circulating water bath. Incubations were stopped by additions of 100% TCA, samples centrifuged to a cell pellet, and nucleic acids and proteins extracted. Ultima Gold scintillation cocktail (Packard) was added to the remnant cellular material in the microcentrifuge tubes, and radiolabeled biochemicals were detected by counting the samples on a scintillation counter.

Bacterial carbon was calculated using a conservative carbon conversion factor of 12.4 fg carbon per cell (Fukuda et al. 1998). To calculate total POC, and in turn, bacterial carbon: total POC, POC was corrected assuming that ~50% of the cells passed through a precombusted Whatman GF/F filter,

$$\text{total POC} = \text{POC} + [0.5 \times \text{bacterial carbon}] \quad (1)$$

Bacterial nitrogen was calculated by dividing bacterial carbon by a bacterial C:N of 4.5 (Goldman and Dennett 1991). Total PN was corrected following Eq. 1. Cell production rates based on thymidine incorporation were calculated using a thymidine conversion factor of 2.4 × 10¹⁸ cells produced per mole thymidine incorporated (Fuhrman and Azam 1982). Specific growth rates (d⁻¹) were derived by dividing the cell production rate (cells L⁻¹ d⁻¹) by the total abundance (cells L⁻¹) as determined by FCM. Bacterial carbon production rates derived from leucine incorporation utilized a leucine conversion factor of 1.5 kg carbon produced per mole leucine incorporated (Simon and Azam 1989). Turnover rates of bacterial biomass were computed by dividing the carbon production rate, P (μg C L⁻¹ d⁻¹), by the bacterial carbon biomass, B (μg C L⁻¹).

To determine mixed layer depth (MLD)-averaged rates, Leu-based BP was integrated through the depth of the mixed layer and divided by its depth. MLD was determined using a criterion of a change of 0.02 from surface σ_t for 1-m binned density measurements. In instances where full water column bacterial data were lacking for integration, an average of abundances and rates measured within the mixed layer were used.

Statistical analysis—Ordinary linear least-squares regression analyses were performed for total and HDNA bacterial abundance, TdR and Leu incorporation, and BP and PP versus time. Model II or geometric mean regression analyses were performed for BP versus PP, size-fractionated PP, size-fractionated chlorophyll *a* (Chl *a*), and POC and PN. Simple linear correlations between bacterial and biological/geochemical variables were also performed. Pearson's product-moment correlation coefficients were calculated, and significance of those correlations was accepted or rejected using an α = 0.05. Statistical comparisons of mean bacterial properties and processes between IN and OUT stations were per-

formed using two-sample *t*-tests (95% confidence interval, $\alpha = 0.05$). Means were computed two ways: by averaging all IN station discrete depth data and comparing to the mean of all OUT station discrete depth data, and by averaging each integrated property over all IN stations and comparing to the mean of all integrated OUT stations.

Primary production, Chl a, and POM—Primary production (PP) measurements were made using H^{14}CO_3 uptake following the methods of Hiscock et al. (2003). Briefly, water was sampled from a trace-metal-clean rosette from depths corresponding to the 100%, 47%, 30%, 16%, and 1% light levels. Water was incubated with H^{14}CO_3 for 24 h in shaded and unshaded, on-deck, flowing seawater incubators, then filtered through various filters for size fractionation (5- and 20- μm polycarbonate filters [Poretics] and a GF/F filter [nominal 0.7- μm pore size]). Radioactivity was determined by liquid scintillation and converted to carbon units using the ambient dissolved inorganic carbon concentrations. Size-fractionated Chl *a* concentrations were measured in nonradioactive water using the same filter types. POM was estimated from samples filtered through GF/F filters and analyzed by pyrolysis in a CHN analyzer. Primary production, Chl *a*, and POM data were MLD averaged as previously described.

Results

North Patch—Iron enrichment positively enhanced primary production (Table 1). Primary production was 140% and 70% higher on days 11 and 39, respectively, than on day 0. IN station PP on day 11 was 43% higher than OUT station PP on day 12. The magnitude of total PP decreased by day 39, but IN station PP remained 40% higher than OUT station PP. While there was an increase in PP between days 0 and 11 in the North Patch, there was no detectable shift in size-fractionated PP. Total PP was dominated by the 0.7–5.0- μm fraction for both IN and OUT stations. A notable shift in size-fractionated PP was observed during the latter stage of our observations. On day 39, the IN station percentages of 5–20- and >20- μm fraction PP were 26% and 26%, respectively, and the 0.7–5.0- μm fraction PP decreased to 48% of total PP. At the OUT station, total PP remained dominated by the 0.7–5.0- μm fraction. Chl *a* also increased over time within the North Patch. Initial Chl *a* concentrations were 0.07 $\mu\text{g L}^{-1}$ and rose to 0.39 and 0.61 $\mu\text{g L}^{-1}$ by days 11 and 39, respectively. Chl *a* concentrations within the iron-enriched waters were also higher than in nonenriched waters.

Heterotrophic bacteria also responded positively to iron enrichment in the North Patch (Table 1). Opportunity to sample the North Patch was limited by ship logistics, so only longer term changes and comparison of enriched and nonenriched waters are presented. IN station bacterial abundance and biomass were 80% greater than OUT station abundance by days 11–12. By day 39, IN station abundance was 170% higher than day 12 OUT station abundance and 110% higher than day 38 OUT station abundance. The net increase in bacterial biomass between days 11 and 39 in the North Patch was 50%. This compares with an apparent net increase in nonenriched waters of 26% over the same time period. The

absolute abundance of HDNA cells was higher for IN stations on days 11 and 39 relative to OUT stations (data not shown); however, the HDNA cells did not change over time in fertilized waters as a fraction of the total abundance.

Thymidine and leucine incorporation rates followed a similar trend to abundance. IN station TdR and Leu on day 11 were twofold higher than OUT station rates. TdR was higher on days 38 and 39 for both IN and OUT stations; but TdR in iron-enriched waters was still higher by a factor 1.5 over nonenriched waters. Incorporation of leucine exhibited little change in both IN and OUT stations late in the bloom; however, IN station Leu remained nearly twofold higher than OUT station rates. The trends for BP were the same as those for Leu because a single conversion factor was used to obtain carbon production. Bacterial production as a percentage of total PP was relatively uniform in time and space.

South Patch—Iron addition also significantly enhanced phytoplankton and bacterial properties in the South Patch. The response to enrichment is summarized by comparison of days 5 and 22 following enrichment (Table 2). Reference OUT stations are an average of four MLD-averaged measurements made on days 7, 9, 13, and 20. Due to the net eastward movement of the iron-fertilized water over time, the reference stations were determined where SF_6 concentrations in the mixed layer reached analytical background. Thus, OUT stations were not temporally consistent and may reflect higher variability than if one nonenriched water mass had been followed over time.

Bacterial abundance and biomass—A significant ($p < 0.05$) increase in bacterial abundance was observed between days 5 and 22 (Table 2, Fig. 1). Abundance and biomass increased by 60%. Variability in OUT station abundance is evident (Fig. 1); however, the change in OUT station abundance over time was not significant. HDNA cell abundance increased steadily between days 5 and 22 (Fig. 1; $p < 0.05$). The percentage of HDNA cells within the South Patch increased from 24% to 45%, whereas the mean of OUT station %HDNA was 36% (Table 2). Least-squares regression of OUT total and HDNA abundance indicated that there were no significant trends over time. A statistical comparison of means at the IN and OUT stations, using discrete depth data, for abundance, HDNA, and biomass showed no statistical differences (*t*-test, $p < 0.05$) (Table 3). However, when days 5 and 8 IN station data were removed from the calculation of the mean, there were significant differences ($p < 0.05$). When the same comparison was made using a computation of the mean with integrated data, no statistical differences were observed (Table 3). Bacterial mortality via microzooplankton grazing and/or viral lysis and/or dilution from surrounding nonenriched waters (0.08 d^{-1} , M. A. Brzezinski pers. comm.) may have accounted for the low observed net increase in bacterial abundance, thus underestimating the gross numerical response.

Bacterial production—Incorporation rates between days 5 and 22 followed the trend of abundance (Table 2, Fig. 2A). TdR increased 3-fold while Leu increased 1.5-fold. Increases in TdR and Leu were significant over time ($p < 0.05$) and

Table 1. North Patch mixed layer depth-averaged stocks and rates of bacteria and phytoplankton. Time denotes days after initial iron fertilization by RV *Revelle*. Days 11 and 12 are averages of two stations inside and outside iron-fertilized waters, respectively. Days 38 and 39 are one station, each. Bacterial production (BP) and primary production (PP) are expressed as $\mu\text{g C L}^{-1} \text{d}^{-1}$. Bold type entries indicate IN stations.

Time	Bacterial abundance (10^8 cells L^{-1})	Bacterial biomass ($\mu\text{g C L}^{-1}$)	Thymidine incorporation ($\text{pmol L}^{-1} \text{h}^{-1}$)	Specific growth rate, $\mu\text{m d}^{-1}$	Leucine incorporation ($\text{pmol L}^{-1} \text{h}^{-1}$)	Bacterial production (BP) ($\mu\text{g C L}^{-1} \text{d}^{-1}$)	%HDNA*
Day 11 IN	7.26	9.01	0.93	0.07	10.1	0.36	35
Day 12 OUT	4.01	4.97	0.44	0.06	4.91	0.18	31
Day 39 IN	10.9	13.5	2.37	0.13	11.0	0.40	35
Day 38 OUT	5.07	6.28	1.54	0.17	5.88	0.21	40
Total PP		PP 0.7–5.0 μm^\ddagger	PP 5–20 μm^\ddagger	PP >20 μm^\ddagger	POC ($\mu\text{g C L}^{-1}$)	PN ($\mu\text{g N L}^{-1}$)	Chl <i>a</i> ($\mu\text{g L}^{-1}$)
Day 0 IN	3.14	2.24 (72%)	0.54 (17%)	0.35 (11%)	43.6	7.75	0.073
Day 11 IN	7.50	5.26 (71%)	1.29 (17%)	0.95 (12%)	39.1	8.04	0.387
Day 12 OUT	4.27	3.76 (88%)	0.38 (9%)	0.13 (3%)	35.9	5.07	0.154
Day 39 IN	5.28	2.56 (48%)	1.35 (26%)	1.37 (26%)	46.0	10.0	0.614
Day 38 OUT	3.20	2.34 (73%)	0.51 (16%)	0.35 (11%)	38.2	7.66	0.334
BP: total PP		BP: 0.7–5.0 μm PP	BP: 5–20 μm PP	BP: >20 μm PP	Bacterial C: total POC ‡	Bacterial N: total PN ‡	
Day 11 IN	0.057±0.35	0.07	0.28	0.38	0.21	0.25	
Day 12 OUT	0.039±0.021	0.05	0.47	1.41	0.13	0.22	
Day 39 IN	0.079±0.056	0.15	0.29	0.29	0.26	0.30	
Day 38 OUT	0.088±0.037	0.09	0.41	0.60	0.15	0.18	

* %HDNA = (HDNA cell count/bacterial abundance) \times 100.

‡ Size-fractionated primary production as a percentage of total primary production is given in parentheses.

‡ Ratios were corrected for bacterial carbon and nitrogen retained on filter (see *Methods*).

Table 2. South Patch mixed layer depth-averaged stocks and rates of bacteria and phytoplankton. Time denotes days after initial iron fertilization by RV *Revelle*. Bacterial production (BP) and primary production (PP) are expressed as $\mu\text{g C L}^{-1} \text{d}^{-1}$. Bold type entries indicate IN stations.

Time	Bacterial abundance (10^8 cells L^{-1})	Bacterial biomass ($\mu\text{g C L}^{-1}$)	Thymidine incorporation ($\text{pmol L}^{-1} \text{h}^{-1}$)	Specific growth rate, $\mu\text{m (d}^{-1}\text{)}$	Leucine incorporation ($\text{pmol L}^{-1} \text{h}^{-1}$)	Bacterial production (BP) ($\mu\text{g C L}^{-1} \text{d}^{-1}$)	% HDNA*
Day 5 IN	3.28	4.07	0.56	0.10	5.37	0.19	24
Day 22 IN	5.25	6.51	1.57	0.17	8.35	0.30	45
Avg. OUT (n=4)	3.43±0.67	4.25±0.83	0.87±0.20	0.15±0.05	4.93±0.83	0.18±0.03	36±8
	Total PP	PP	PP	PP	POC	PN	Chl <i>a</i>
		0.7–5.0 μm^\dagger	5–20 μm^\dagger	>20 μm^\dagger	($\mu\text{g C L}^{-1}$)	($\mu\text{g N L}^{-1}$)	($\mu\text{g L}^{-1}$)
Day 0 IN	7.41	3.99 (54%)	1.26 (17%)	2.15 (29%)	75.1	14.9	0.13
Day 5 IN	7.17	3.34 (47%)	0.90 (13%)	2.93 (40%)	90.7	19.2	0.61
Day 22 IN	10.5	3.08 (30%)	2.75 (27%)	4.49 (43%)	168	38.5	3.61
Avg. OUT	4.25±1.07	1.48 (35%)	0.60 (14%)	2.17 (51%)	74.8±6.02	15.5±1.58	0.44±0.07
	BP: total PP	BP: 0.7–5.0 μm	BP: 5–20 μm	BP: >20 μm	Bacterial C: total POC [‡]	Bacterial N: total PN [‡]	
Day 5 IN	0.022±0.009	0.06	0.21	0.07	0.07	0.05	
Day 22 IN	0.010±0.004	0.10	0.11	0.07	0.04	0.04	
Avg. OUT	0.049±0.019	0.12	0.30	0.08	0.06	0.06	

* % HDNA = (HDNA cell count/bacterial abundance) × 100.

† Ratios were corrected for bacterial carbon and nitrogen retained on filter.

‡ Size-fractionated primary production as a percentage of total primary production is given in parentheses.

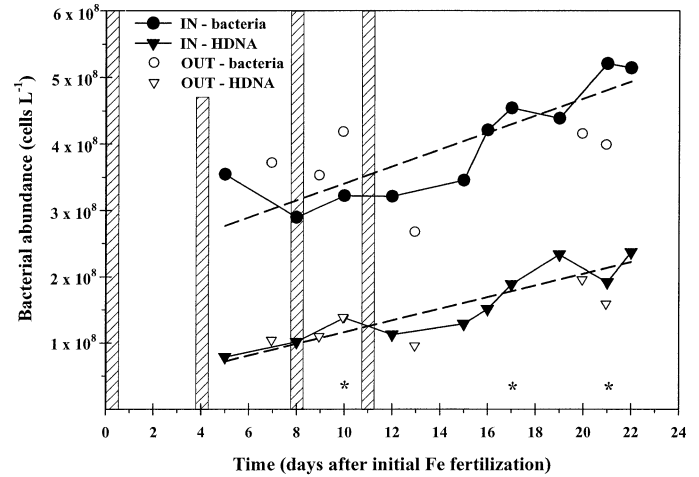


Fig. 1. South Patch total bacterial abundance, IN stations (filled circles; $r^2 = 0.72$, $p < 0.05$), and high DNA-containing cell abundance (HDNA) (filled triangles; $r^2 = 0.81$, $p < 0.05$). OUT stations are denoted by open circles and open triangles. Asterisks denote transect stations where an average of 10-m abundance was calculated. Hashed areas denote iron enrichment by RV *Revelle*. Dashed lines denote linear least-squares regressions of IN station abundances.

depth-averaged (integrated) IN station TdR and Leu were higher than depth-averaged OUT station rates. Mean OUT station TdR and Leu were comparable to day 5 rates. However, IN station TdR and Leu were higher than OUT station rates by day 22 (Table 2). Significant differences between mean IN and OUT station TdR and Leu (t -test, $p < 0.05$) were apparent for two separate estimates of the mean (average of all discrete depth data and average of all integrated data) with the exception of IN versus OUT, days 5–22 integrated TdR (Table 3). Cell-specific incorporation of thymidine (SpTdR) and leucine (SpLeu) were highly variable for both IN and OUT stations, with neither SpTdR nor SpLeu showing any clear trends (Fig. 2B). SpLeu IN was significantly different from OUT and peaked on days 12 and 21 within iron-enriched waters. Periodic maxima in specific incorporation rates may indicate episodes of enhanced growth in response to iron addition on days 8 and 11. Bacterial production doubled from 0.2 to 0.4 $\mu\text{g C L}^{-1} \text{d}^{-1}$ (Fig. 3A). OUT station BP averaged 0.2 $\mu\text{g C L}^{-1} \text{d}^{-1}$ and was consistently less than IN station BP over the course of 17 d.

Primary production in the South Patch increased fourfold over 17 d (Fig. 3A). The increase over time was not statistically significant ($p > 0.05$); however, when the final time point is excluded, the relationship becomes significant ($p < 0.05$). A shift in the size distribution of PP was also observed within the South Patch as PP in the 5–20- μm fraction increased from 17% to 27% of total PP from days 0 to 21 (Table 2). The relative percentage of the total PP < 5 μm decreased from 54% to 30%, whereas the %PP in the >20- μm fraction increased from 29% to 43% by day 21. Fifty-one percent of the average of OUT station PP was in the >20- μm fraction. Despite the larger relative increase in PP, BP was closely correlated with total PP (Fig. 3B). Geometric mean regression revealed that 80% of the variation in BP

Table 3. Two-sample *t*-test results of IN versus OUT station bacterial properties in the South Patch. Statistical significance was based on the criteria of a 95% confidence interval and an $\alpha = 0.05$. NS denotes comparisons that were not statistically significant. Sample sizes are denoted for both IN and OUT stations in parentheses.

Bacterial property or process	Mean, all IN stations* days 5–22 ($n_{in}=32, n_{out}=20$)	Mean, all IN stations* days 8–22 ($n_{in}=27, n_{out}=20$)	Mean, all IN stations* days 12–22 ($n_{in}=22, n_{out}=20$)	Mean, all integrated IN stations† days 5–22 ($n_{in}=7, n_{out}=4$)	Mean, all integrated IN stations† days 8–22 ($n_{in}=6, n_{out}=4$)	Mean, all integrated IN stations† days 12–22 ($n_{in}=5, n_{out}=4$)
Abundance	NS	$p = 0.047$	$p = 0.0037$	NS	NS	NS
Biomass	NS	$p = 0.047$	$p = 0.0037$	NS	NS	NS
HDNA abundance	NS	$p = 0.017$	$p = 0.0018$	NS	NS	NS
TdR	$p = 0.0025$	$p = 0.0000$	$p = 0.0000$	NS	$p = 0.015$	$p = 0.023$
Leu	$p = 0.0000$	$p = 0.0000$	$p = 0.0000$	$p = 0.028$	$p = 0.015$	$p = 0.0051$

* Means were calculated by averaging all IN station discrete depth data for the specified time period and comparing the mean of all OUT station data.

† Means were calculated by averaging all integrated IN station data for the specified time period and comparing the mean of all integrated OUT stations.

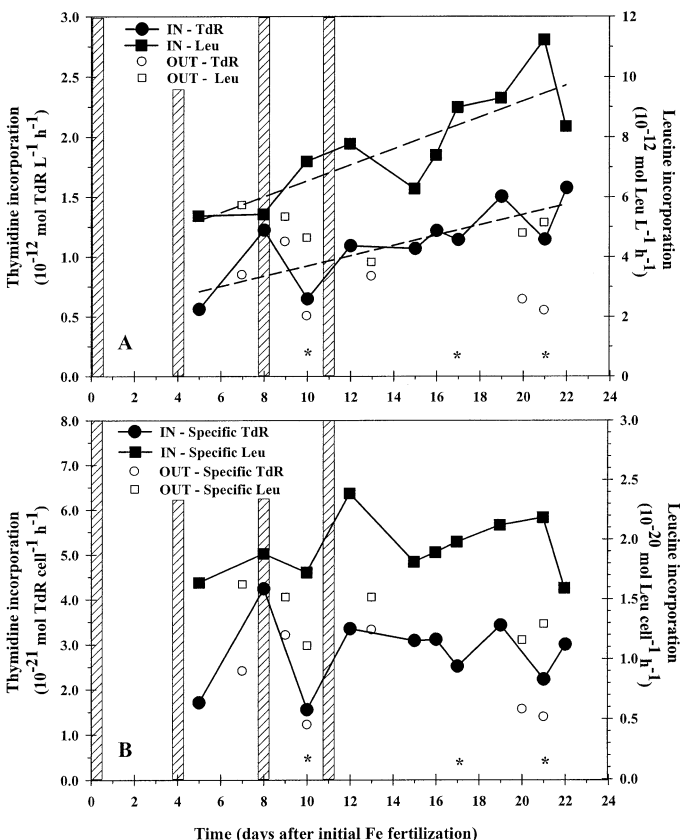


Fig. 2. (A) South Patch volumetric incorporation rates of thymidine (TdR; filled circles, $r^2 = 0.53$, $p = 0.01$) and leucine (Leu; filled squares, $r^2 = 0.63$, $p < 0.05$). Open circles and open squares denote OUT station TdR and Leu incorporation rates, respectively. (B) South Patch cell-specific TdR (not significant) and Leu incorporation (not significant) rates. Rates are normalized to total bacterial abundance. Asterisks denote transect stations where an average of 10-m rates was calculated. Hashed areas denote iron enrichment by RV *Revelle*. Dashed lines denote linear least-squares regressions.

was attributed to variability in total PP, demonstrating that BP and PP were thus closely coupled. However, BP was only 1% of PP (Fig. 3B) and 3% of PP on days 5 and 22 (Table 2).

Stocks of Chl *a*, POC, and PN also increased as a result of iron enrichment (Table 2). Chl *a* increased from 0.1 to 3.6 $\mu\text{g L}^{-1}$ between days 0 and 21. Particulate organic carbon and nitrogen both increased more than twofold over this period. Bacterial production was strongly correlated to total Chl *a* (Fig. 5A; $r = 0.86$, Table 4) and correlated most strongly with the $>20\text{-}\mu\text{m}$ fraction (Fig. 5A; $r = 0.94$, Table 4) and less strongly with the $5\text{--}20\text{-}\mu\text{m}$ fraction (Fig. 5A; $r = 0.73$, Table 4). BP was also significantly correlated to PN (Fig. 5B; $r = 0.77$, Table 4). Bacterial abundance correlated significantly with Chl *a*, but did not correlate significantly with POC, PN, or PP (Table 4). Bacterial biomass, as a fraction of total POC and PN, decreased from day 5 to 22 (Table 2). The decrease of bacterial carbon : total POC is most likely a dilution effect due to the larger increase in autotrophic biomass relative to bacterial biomass (600% vs. 50%).

Bacterial growth rates—Bacterial community growth rates were estimated by growth in dilution culture and cell-specific ^3H -TdR incorporation. IN station TdR-based growth rates were equal to OUT station rates during the early and middle stages of the bloom (Table 5). Only late in the experiment was the TdR-based growth rate higher than its reference OUT station. Perhaps more relevant is the temporal increase in TdR-based growth rate within the South Patch. TdR-based growth rate increased from 0.14 d^{-1} (days 5–7) to 0.19 d^{-1} (day 12). The same trend was observed in the dilution experiments. The bacterial growth rate increased from 0.16 d^{-1} (days 5–7) to 0.19 d^{-1} (day 12), but growth was balanced by mortality (Table 5). By day 19, growth rate increased further to 0.29 d^{-1} , nearly doubling since day 7, and exceeded mortality (-0.06 d^{-1}). Growth rates in OUT stations were higher than at IN stations, except late in the experiment, where they were nearly equal. OUT station growth rates were also higher than the rates of mortality, suggesting either low grazer/viral activity and/or actively growing bacteria in nonenriched waters. Indeed, nearly a third of the bacterial population in OUT stations were HDNA cells, further suggesting an actively growing sub-

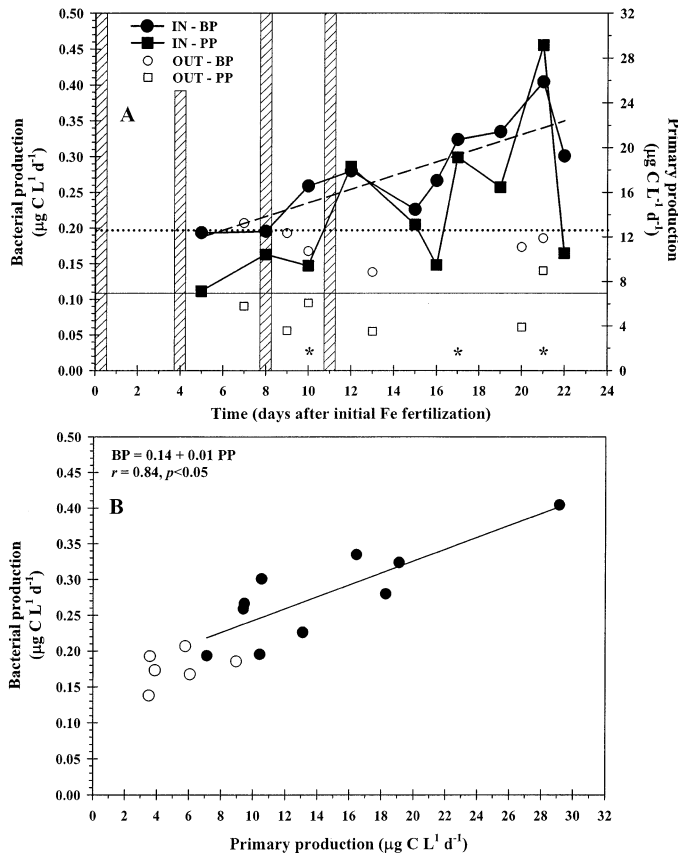


Fig. 3. (A) South Patch bacterial (filled circles, $r^2 = 0.63$, $p < 0.05$) and primary production (filled squares, $r^2 = 0.23$, not significant). Open circles and open squares denote OUT station bacterial production and primary production, respectively. Dashed regression lines represent ordinary linear least-squares regressions of BP versus time. The solid horizontal line represents the level of PP at time zero. The dotted horizontal line represents the level of BP at time zero following the model II (geometric mean) regression in panel B. Hatched areas denote iron enrichment by RV *Revelle*. Asterisks denote transect stations where an average of 10-m rates was calculated. (B) Model II regression of bacterial versus primary production from all IN stations (filled circles) in the South Patch. OUT stations are denoted by open circles.

population (Table 2). Perhaps of more relevance is the temporal increase in growth rates evident from the dilution experiments within iron-enriched waters. While the absolute magnitudes of the dilution-based growth rates were higher compared with TdR-based estimates, the trends for the two independent measures of growth rate were the same: an increase in the growth rate from early to late in the enrichment.

Discussion

Heterotrophic bacterial dynamics during SOFeX—Following iron fertilizations north and south of the APFZ, BP increased as we expected. The magnitude of the increase (twofold), however, was less than that observed by Hall and Safi (2001) during SOIREE and Cochlan (2001) in the Equatorial Pacific Ocean during IronEx II. In these studies, bacteria responded to iron enrichment with a threefold increase

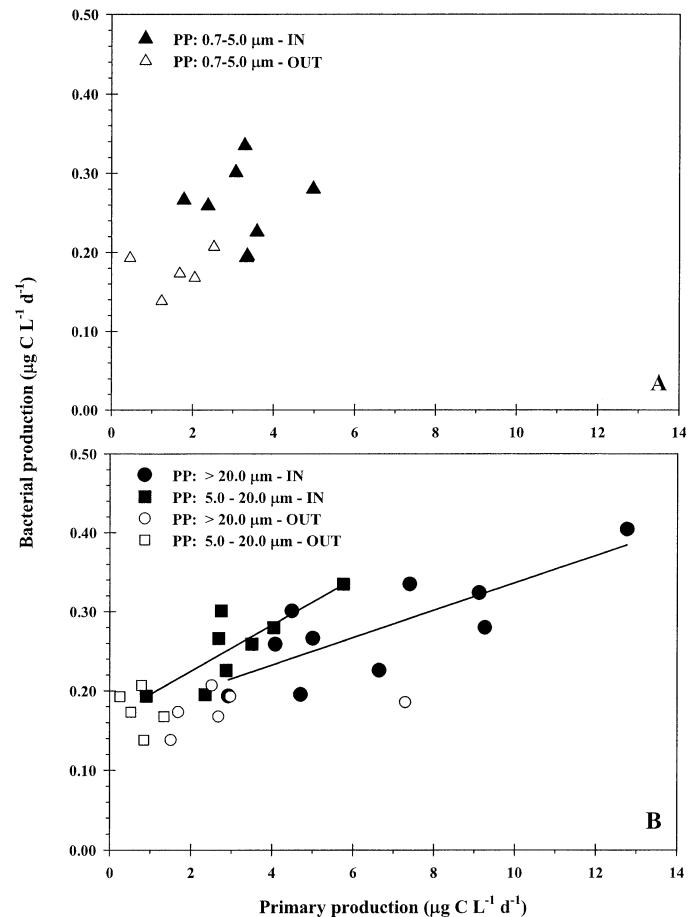


Fig. 4. (A) Model II regression of bacterial production versus 0.7–5.0- μm -size fraction primary production (not significant) from all IN stations in the South Patch. OUT stations are denoted by open symbols. (B) Model II regression of bacterial production versus 5.0–20- μm (filled squares, $r = 0.82$, $p < 0.05$) and >20- μm (filled circles, $r = 0.82$, $p < 0.05$) size fraction primary production from IN stations in the South Patch. Respective OUT stations for each size fraction of primary production are denoted by open symbols.

in BP. Contrary to our expectation that bacterial abundance would not increase, we observed a twofold net accumulation of bacterial biomass over the course of 40 d in the North Patch and 22 d in the South Patch. This is in contrast with the observations of Hall and Safi (2001), who saw no net accumulation in biomass over 13 d, but is consistent with those of Cochlan (2001), who saw a similar net increase over 14 d in tropical waters. During IronEx II in the equatorial Pacific, Landry et al. (2000) calculated a net accumulation rate for heterotrophic bacteria of 0.08 d^{-1} . Furthermore, we observed a net increase in HDNA cells in the South Patch. This suggests an actively growing subpopulation of bacteria (Lebaron et al. 2001) and is corroborated by TdR data.

Enhancement of bacterial growth in iron-fertilized waters is evident from the independent estimates of growth rate. The specific growth rate, as measured by ^3H -TdR incorporation, showed a modest increase over time. Cochlan (2001) observed an increase in the specific growth rate using ^3H -

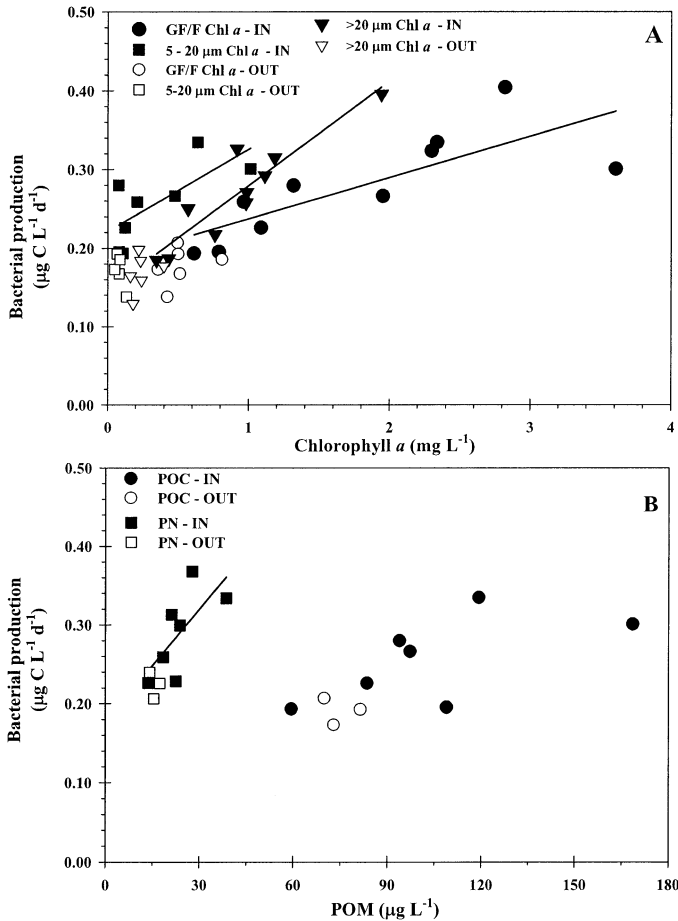


Fig. 5. (A) Model II regression of bacterial production versus total fluorometric chlorophyll *a* (filled circles, $r = 0.79$, $p < 0.05$), 5–20- μm fluorometric Chl *a* (filled squares, $r = 0.72$, $p < 0.05$), and >20- μm fluorometric Chl *a* (filled triangles, $r = 0.92$, $p < 0.05$) from all IN stations in the South Patch. Respective OUT stations for each size fraction of fluorometric Chl *a* are denoted by open symbols. (B) Model II regression of bacterial production versus particulate organic carbon (POC; filled circles, $r = 0.63$, not significant), and particulate organic nitrogen (PN; filled squares, $r = 0.70$, not significant), from all IN stations in the South Patch. Respective OUT stations for POC and PN are denoted by open symbols.

Table 5. Specific growth rates of heterotrophic bacteria in the South Patch.

Location in South Patch	Day	Dilution,* μ (d^{-1})	TdR,† μ (d^{-1})
IN	0	0.22 (–0.24)	—
IN (early)‡	5–7	0.16 (–0.15)	0.14
IN (middle)‡	12	0.19 (–0.23)	0.19
IN (late)‡	19	0.29 (–0.06)	0.19
OUT	7	0.26 (–0.18)	0.14
OUT	13	0.29 (–0.21)	0.19
OUT	21	0.26 (–0.19)	0.09

* Growth and mortality rates (parentheses) from dilution experiments, courtesy of M. Landry and S. L. Brown.

† Mixed layer depth-averaged TdR was used to calculate growth rates. Bold type indicates IN stations.

‡ Stage of the iron-induced phytoplankton bloom. All growth rates were significantly greater than zero ($p < 0.05$).

Leu from 0.10 to 0.45 d^{-1} following iron enrichment. The microzooplankton dilution experiments also showed an increase in the community growth rate over time, with bacterial growth exceeding mortality by the end of the experiment.

Comparison of bacterial dynamics between the North and South Patches is limited by the paucity of observations in the North Patch and the lack of time-zero measurements. However, a comparison can be made between the two experiments' responses to iron enrichment assuming that OUT stations were similar to initial conditions. By day 11 in the North Patch, bacterial biomass had nearly doubled, whereas there was no change in biomass by day 12 in the South Patch. Incorporation rates in the North Patch had doubled by day 11, with the same change in TdR and a slightly lower increase in Leu in the South Patch. Thymidine-based growth rate did not change substantially in either the North or South Patches after 11 and 12 d, respectively.

The bacterial response during SOFeX was also consistent with previous mesoscale enrichments in terms of the relative proportion of biomass (BB:PB) and the correlation of BP to PP. We observed a disproportionate increase between phytoplankton and bacterial biomass. Using Chl *a* as a proxy for phytoplankton biomass, North Patch phytoplankton bio-

Table 4. Simple linear correlations of bacterial production and abundance versus size-fractionated chlorophyll *a* (Chl *a*), POC, PN, and size-fractionated primary production in the South Patch. + denotes statistically significant correlations at $p < 0.05$. – denotes nonsignificant correlations.

Bacterial production versus	$p < 0.05$	Correlation coefficient (r)	Bacterial abundance versus	$p < 0.05$	Correlation coefficient (r)
GF/F Chl <i>a</i>	+	0.79	GF/F Chl <i>a</i>	+	0.94
0.7–5.0 μm Chl <i>a</i>	+	0.65	0.7–5.0 μm Chl <i>a</i>	+	0.91
5.0–20 μm Chl <i>a</i>	+	0.72	5.0–20 μm Chl <i>a</i>	+	0.96
>20 μm Chl <i>a</i>	+	0.92	>20 μm Chl <i>a</i>	+	0.80
POC	–	0.63	POC	–	0.71
PN	–	0.70	PN	+	0.79
Primary production	+	0.84	Primary production	–	0.51
0.7–5.0 μm PP	–	–0.01	0.7–5.0 μm PP	–	–0.32
5.0–20 μm PP	+	0.82	5.0–20 μm PP	–	0.19
>20 μm PP	+	0.80	>20 μm PP	–	0.44

mass increased eightfold compared with a twofold increase in bacterial biomass over 40 d. In the South Patch, Chl *a* increased 27-fold compared with a 2-fold increase in bacterial biomass. Cochlan (2001) observed the same trend, with a peak increase in phytoplankton biomass of 17-fold with only a 2-fold increase in bacterial biomass. Hall and Safi (2001) observed a peak increase in integrated Chl *a* of sixfold with no increase in bacterial biomass. A proximal cause for this disproportionate increase in biomass is a high rate of bacterial mortality relative to phytoplankton mortality and a closer coupling between bacteria and their predators. In fact, bacterial mortality during SOFeX could have balanced growth or allowed only minor accumulation of biomass (M. R. Landry et al. pers. comm.). Increases in heterotrophic nanoflagellates and the uncoupling of BB from BP during SOIREE were evidence of a high rate of bacterial mortality (Hall and Safi 2001).

Likewise, bacterial growth efficiency (BGE) may have been unaffected or may have decreased in response to the increase in PP. For example, if BGE decreased, then less carbon would be diverted to creating biomass, resulting in a higher proportion of carbon being respired. This would result in the observed disproportionate increase in phytoplankton biomass relative to bacterial biomass. Because bacterial respiration rates were not measured, estimates of BGE are not available and we cannot rule out this possibility. We can point to the observation that bacterial carbon production in the South Patch was significantly correlated to net particulate primary production (PP) as circumstantial evidence toward ruling out the effect of BGE on the lower relative increase in bacterial biomass. Hall and Safi (2001) found a similar positive correlation between BP and PP. The relationship we observed between the two parameters is striking ($r = 0.80$) and both BP and PP trends were similar in time and space. This suggests that bacteria were responding positively to PP and, in turn, creating new biomass. Del Giorgio and Cole (2000) showed that BGE generally increases as BP increases and also reported that BGE is proportional to PP. In this case, a potential decrease in BGE in response to higher BP and PP during SOFeX would run counter to these findings.

We assumed a priori that the majority of the prokaryotic response during SOFeX would be by heterotrophic bacteria. Our abundance measurements may more accurately reflect the response of the full prokaryotic community (*Bacteria* and *Archaea*) and not exclusively heterotrophic bacteria. Members of *Archaea* may have contributed to the heterotrophic response we observed. We plan to investigate their relative abundance and prokaryotic diversity in future studies.

Substrate limitation: the case for carbon—During SOFeX, the first component of the biological pump, primary production, was unequivocally stimulated by multiple iron additions (Fig. 3). Drawdown of inorganic nutrients (DIC, NO_3 , and PO_4), a response observed in previous experiments, was also observed. While the evidence for iron limitation of phytoplankton during SOFeX is unequivocal, the argument for iron limitation of heterotrophic bacteria is not as clear.

First, bacterial incorporation rates increased over time in the low iron ($<1 \text{ nmol L}^{-1}$) OUT stations in the North Patch (Table 1). Also, TdR-specific growth rate was higher in non-

enriched waters by day 38 and higher than the growth rate measured in the North Patch on day 39. Leucine incorporation, an indicator of biomass synthesis, was higher by 20% on day 38 compared with day 12 in the reference stations outside the North Patch. If one assumes that iron directly limits bacterial growth, then the observed higher TdR and Leu in low-iron OUT stations over time and relative to IN stations are paradoxical.

Second, BP in the South Patch showed a lag of approximately 8 d behind the initial enrichment with iron and was initiated after three enrichments with iron (Fig. 3A). Primary production, on the other hand, appears to increase after 5 d, with shifts in size-fractionated PP to larger cells (Table 2). We assume that BP at time zero in the South Patch was similar to that of OUT station BP and BP on day 5. In fact, using the Model II regression of BP and PP (Fig. 3B) and calculating BP using a time zero PP of $7.4 \mu\text{g C L}^{-1} \text{ d}^{-1}$, BP is computed to be $0.2 \mu\text{g C L}^{-1} \text{ d}^{-1}$, nearly the same as day 5 in iron-fertilized waters. Considering heterotrophic bacteria have a high iron demand (Tortell et al. 1996) and are highly competitive in taking up iron compared with phytoplankton (Hutchins et al. 1999), it is doubtful that in an iron-limited system heterotrophic bacterial growth would lag behind phytoplankton growth following new inputs of iron, if iron were the primary control on bacterial growth.

Third, growth rates estimated by ^3H -TdR incorporation and from dilution experiments from low-iron reference stations outside the South Patch are comparable with those in iron-fertilized waters. If heterotrophic bacteria were iron-limited in the Southern Ocean like phytoplankton, we would expect to see lower growth rates in the OUT stations. Furthermore, growth rates exceeded mortality rates in several OUT stations. We note, however, that there were systematic differences between the experimental conditions of two growth-rate estimates.

Given the paucity of iron, how are heterotrophic bacteria able to grow in non-iron-fertilized waters? As mentioned above, heterotrophic bacteria are highly competitive with phytoplankton for iron due to their ability to acquire iron by expressing iron-binding ligands known as siderophores (Butler 1998). Heterotrophic bacteria are capable of acquiring iron using their own expressed siderophores and have been shown to acquire iron by utilizing exogenous siderophores as well (Hutchins et al. 1999). Thus, siderophore-mediated iron uptake is one possible way in which heterotrophic bacteria likely circumvented iron limitation during SOFeX. It would explain the comparable growth rates from seawater cultures and rates of substrate incorporation we observed inside and outside the North and South Patches. Another possibility is the acquisition of iron bound to bulk DOM. The majority ($>99\%$) of dissolved iron in the ocean has been found to be organically complexed (Rue and Bruland 1997), a pool that is poorly characterized. It is possible that heterotrophic bacteria are capable of acquiring iron from bulk DOM using strategies that are currently unknown.

The exclusion of iron as a limiting factor leaves macronutrients and organic carbon as potential growth-limiting factors. Macronutrients (nitrate and phosphate) were replete throughout the experiment and ammonium concentrations increased in iron-fertilized waters, although the concentra-

tions remained low ($0.1\text{--}0.2 \mu\text{mol L}^{-1}$) (Cochlan pers. comm.). Thus, dissolved organic carbon limitation likely constrained bacterial growth. There are numerous sources of DOM to bacteria within ocean food webs, and it is produced through a variety of mechanisms (Nagata 2000). DOM composition and lability (Carlson 2002) exhibits a wide range, and these (rather than DOM concentration) directly affect heterotrophic bacterial growth. In the open ocean, one source of DOM to bacteria is extracellular release by phytoplankton (ER; Nagata 2000; Carlson 2002). ER varies as a function of light, nutrient availability, and species composition (Nagata 2000). Despite its variation over ocean systems, ER tends to be linearly related to PP and averages 13% of PP (Baines and Pace 1991). We can demonstrate that direct excretion by phytoplankton during SOFeX was sufficient to meet bacterial carbon demand (BCD) and alleviate carbon limitation. First, we assumed a conservative value for bacterial growth efficiency (BGE) of 20% (Carlson et al. 1999; Ducklow et al. 2000). Next, we employed averaged BP from OUT stations and day 22 IN station (Table 2) to calculate BCD. Finally, we assumed a constant ER of 13% over time using PP concurrent with BP (Table 2). In nonenriched waters, ER could meet only 60% of BCD. By difference, this means that 40% of BCD was met by other carbon sources. In fertilized waters on day 22, ER could meet 95% of BCD, thus obviating bacterial need for other carbon sources. Because PP was elevated above $8 \mu\text{g C L}^{-1} \text{d}^{-1}$ in the South Patch after day 6 (Fig. 3A), it is likely that ER provided a constant and sufficient source of carbon to bacteria during the bloom. The close association of BP to PP and to size-fractionated PP ($5\text{--}20$ and $>20 \mu\text{m}$) (Figs. 3, 4) supports the argument that heterotrophic bacteria were indeed reliant upon freshly produced photosynthate. Results for other values of BGE are listed in Table 6.

With the exception of one study in the Antarctic (Pakulski et al. 1996), field observations of iron limitation of heterotrophic bacteria are scarce. To date, most evidence supports DOM limitation across a range of ocean systems: the sub-Arctic and equatorial Pacific Ocean (Kirchman 1990), the northwest Atlantic Ocean (Carlson et al. 2002), and the Southern Ocean (Carlson et al. 1998; Hall and Safi 2001; Ducklow 2003). Nutrient amendment experiments carried out in the Southern Ocean (Church et al. 2000) and off the coast of California (Kirchman et al. 2000) suggested a co-limitation of bacterial growth by iron and DOM. Iron and carbon (as amino acids or glucose) in these studies stimulated bacterial growth above carbon alone. Tortell et al. (1996) illustrated the dynamic interplay between iron and DOM limitation. They measured growth efficiencies of bacterial isolates in culture under iron-replete and -depleted conditions and found reduced growth efficiencies under iron limitation. The implication was that carbon flow through the microbial food web could be altered such that bacteria could serve as carbon sinks or carbon links to higher trophic levels as a function of iron availability, assuming that carbon is not limiting. Whether this occurs in natural environments remains an open question.

While our results lead us to the conclusion that heterotrophic bacteria were carbon limited during SOFeX, we emphasize two caveats regarding nutrient limitation of hetero-

Table 6. Estimation of the fraction of bacterial carbon demand hypothetically supported by phytoplankton extracellular release. BGE, bacterial growth efficiency; BP, bacterial production ($\mu\text{g C L}^{-1} \text{d}^{-1}$); BCD, bacterial carbon demand ($\mu\text{g C L}^{-1} \text{d}^{-1}$); PP, particulate primary production ($\mu\text{g C L}^{-1} \text{d}^{-1}$); PER, extracellular release, expressed as a percent of the estimated primary production. Assumed values of BGE are listed. BP and PP are from averaged OUT stations and day 22 IN station (Table 3). BCD is calculated as BP BGE^{-1} . PER is fixed at 13% of PP (Baines and Pace 1991). The fraction of BCD supported by PER is calculated as PER BCD^{-1} . Bold type indicates IN stations.

Location	BGE	BP	BCD	PP	PER	Fraction of BCD supported by PER (%)
OUT	0.10	0.18	1.80	4	0.52	29
	0.15	0.18	1.20	4	0.52	43
	0.20	0.18	0.90	4	0.52	58
	0.25	0.18	0.72	4	0.52	72
	0.30	0.18	0.60	4	0.52	87
IN	0.10	0.30	3.00	11	1.43	48
	0.15	0.30	2.00	11	1.43	72
	0.20	0.30	1.50	11	1.43	95
	0.25	0.30	1.20	11	1.43	119
	0.30	0.30	1.00	11	1.43	143

trophic bacteria. First, we do not claim widespread carbon limitation across the Southern Ocean nor do we exclude iron limitation elsewhere in the Southern Ocean at other times. The Southern Ocean encompasses a range of ecological provinces that possess dynamic food-web structures and nutrient regimes. Thus, we suggest caution in making broad generalizations regarding nutrient limitation of heterotrophic bacteria in the Southern Ocean. Second, we cannot say with certainty that all members of the prokaryotic community experienced nutrient/substrate limitation. The methods employed in this study restrict interpretations to the bulk community of prokaryotes and the members of that community that are capable of assimilating radiolabeled organic substrates. Therefore, it is possible that subpopulations of prokaryotes do in fact experience iron or carbon limitation.

Carbon cycle implications—SOFeX provided an opportunity to study the role of heterotrophic bacteria in the carbon cycle during a phytoplankton bloom. The blooms initiated during SOFeX are not unlike others that occur in the Southern Ocean and elsewhere throughout the year. Heterotrophic bacterial remineralization is an important component of the ocean carbon cycle because it prevents net community production from approaching gross carbon production. This occurs through the remineralization of DOC, a pool that would otherwise accumulate or be exported by deep ocean convection. DOC production during phytoplankton blooms is a consistent phenomenon (Carlson et al. 1998) and its flow into the microbial food web has been well documented (Landry et al. 2000).

Several features of the bacterial response during SOFeX are consistent with blooms elsewhere in the Southern Ocean. Carlson et al. (1998) found that 90% of the organic carbon

produced during the spring bloom in the Ross Sea accumulated as POC and the remaining 10% as DOC. They reasoned that little DOC accumulated as a result of bacterial utilization and that 72% of the supply of freshly produced DOC fueled bacterial growth. Ducklow (2003) and Carlson and Hansell (2003) recently reviewed bacterial dynamics and DOM dynamics, respectively, in the Ross Sea. Collectively, the authors found that semilabile DOM at near Redfield stoichiometry accumulated in the Ross Sea during the austral spring with almost complete removal by the onset of winter due to bacterial remineralization.

The net accumulation of bacterial biomass is another feature observed in the Ross Sea. Ducklow et al. (2001a) observed an order of magnitude net increase in bacterial biomass in the upper water column over the course of the spring and summer at a net rate of 0.03 d^{-1} . This is surprisingly close to the net increase we observed in our study, 0.02 d^{-1} . Despite the large accumulation of bacterial biomass, the authors concluded that bacterial mortality remained a significant process over the same timescale such that two thirds of bacterial carbon was transferred through the microbial food web. We suggest that similar resource–predator–prey dynamics occurred during SOFeX considering the comparable growth and mortality rates estimated by microzooplankton dilution experiments. Ducklow et al. (2001a) also found BP to comprise a small fraction of PP (1–10%), with increases in the ratio from spring to summer. Our finding that BP was only 1% of PP is in line with their observation; however, it is possible that the BP:PP ratio might have similarly been more dynamic during the declining stage of the bloom (Ducklow et al. 2002). A prolonged observation of an iron-induced bloom is needed in the future to more fully characterize the response of heterotrophic bacteria.

In addition to the effects on dissolved and particulate organic carbon flows, heterotrophic bacteria can indirectly affect silica and iron cycle dynamics. Silica is a key element in diatom frustules and is known to limit new production in HNLC waters. The concentration of bioavailable silicate (Si(OH)_4) in the upper ocean reflects the balance between vertical fluxes of the two pools, production of biogenic silica (bSiO_2), and its dissolution. Recently, evidence has emerged that heterotrophic bacterial activity could accelerate the rate of bSiO_2 dissolution through hydrolytic enzymatic degradation of protective organic coatings around diatom frustules (Bidle et al. 2003). The implication from these studies is that the efficiency of the silicate pump would decrease, in turn, permitting a higher degree of production that was based on recycled silicate. This mechanism could have implications for DIC removal in low silicate HNLC regions like the North Patch in SOFeX. It is possible that heterotrophic bacteria played a role in maintaining silicate supply and, in turn, new production by diatoms through the mechanism described above. This type of positive feedback mechanism (PP stimulating BP, which then enhances Si recycling, further enhancing PP and so forth) may be an important factor in the persistence of phytoplankton blooms and carbon export. Other mechanisms such as introduction of high silicate waters (upwelling or diverging water masses) may have also contributed to the observed diatom dominance.

Iron cycling within the plankton food web during SOFeX

may have also played a role in both blooms' dynamics. As is the case with carbon, iron can be cycled through the microbial food web (Tortell et al. 1999). During IronEx II, microzooplankton biomass (heterotrophic nanoflagellates and dinoflagellates, ciliates) increased over the course of the iron-enriched bloom (Landry et al. 2000) with microzooplankton grazing occurring across phytoplankton taxa with particularly efficient removal of diatoms. They also suggested that an efficient recycling of iron and silicate allowed phytoplankton growth rates to remain high. The plankton food web can also be an important source to the dissolved and particulate iron pools (Hutchins et al. 1993). It is unclear whether heterotrophic bacteria would be important sources or sinks of iron. They may represent a significant source of recycled iron to phytoplankton based on their high intracellular Fe:C relative to phytoplankton (Tortell et al. 1996), but this may be dependent on the activity and composition of the microbial food web as well as the composition and rate of supply of iron to the dissolved pool. Clearly, more work is needed to more completely elucidate the role of heterotrophic bacteria in modifying carbon, silica, and iron dynamics.

The heterotrophic bacterial response during SOFeX is both similar to and in contrast with previous open-ocean iron-enrichment experiments. The differences between our study and previous ones likely reflect subtle differences in the initial structure and composition of the microbial food web. The increase in bacterial production to new inputs of organic carbon, accelerated growth rate, and high bacterial mortality appear to be consistent features of in situ iron enrichment. These features are also consistent with previous studies describing bacterioplankton dynamics during phytoplankton blooms in the ocean. The contribution of heterotrophic bacterial processes, while quantitatively less than that of phytoplankton, remains a poorly studied, albeit critical, component of the carbon cycling of iron-stimulated blooms.

References

- BAINES, S. B., AND M. L. PACE. 1991. The production of dissolved organic matter by phytoplankton and its importance to bacteria: Patterns across marine and fresh-water systems. *Limnol. Oceanogr.* **36**: 1078–1090.
- BAKKER, D. C. E., A. J. WATSON, AND C. S. LAW. 2001. Southern Ocean iron enrichment promotes inorganic carbon drawdown. *Deep-Sea Res. II* **48**: 2483–2507.
- BIDIGARE, R. R., AND OTHERS. 1999. Iron-stimulated changes in ^{13}C fractionation and export by equatorial Pacific phytoplankton: Toward a paleogrowth rate proxy. *Paleoceanography* **14**: 589–595.
- BIDLE, K. D., M. A. BRZEZINSKI, R. A. LONG, J. L. JONES, AND F. AZAM. 2003. Diminished efficiency in the oceanic silica pump caused by bacteria-mediated silica dissolution. *Limnol. Oceanogr.* **48**: 1855–1868.
- BUTLER, A. 1998. Acquisition and utilization of transition metal ions by marine organisms. *Science* **281**: 207–210.
- CARLSON, C. A. 2002. Production and removal processes, p. 91–151. *In* D. A. Hansell and C. A. Carlson [eds.], *Biogeochemistry of marine dissolved organic matter*. Elsevier.
- , N. R. BATES, H. W. DUCKLOW, AND D. A. HANSELL. 1999. Estimation of bacterial respiration and growth efficiency in the Ross Sea, Antarctica. *Aquat. Microb. Ecol.* **19**: 229–244.

- , H. W. DUCKLOW, D. A. HANSELL, AND W. O. SMITH, JR. 1998. Organic carbon partitioning during spring phytoplankton blooms in the Ross Sea polynya and the Sargasso Sea. *Limnol. Oceanogr.* **43**: 375–386.
- , AND OTHERS. 2002. Effects of nutrient amendments on bacterioplankton production, community structure, and DOC utilization in the northwestern Sargasso Sea. *Aquat. Microb. Ecol.* **30**: 19–36.
- , AND D. A. HANSELL. 2003. The contribution of dissolved organic carbon and nitrogen to the biogeochemistry of the Ross Sea. *In* G. DiTullio and R. B. Dunbar [eds.], *Biogeochemistry of the Ross Sea*. *Ant. Res. Ser.* **78**: 123–142.
- CHISHOLM, S. W., P. G. FALKOWSKI, AND J. J. CULLEN. 2001. Discrediting ocean fertilization. *Science* **294**: 309–310.
- CHURCH, M. J., D. A. HUTCHINS, AND H. W. DUCKLOW. 2000. Limitation of bacterial growth by dissolved organic matter and iron in the Southern Ocean. *Appl. Environ. Microbiol.* **66**: 455–466.
- COALE, K. H., AND OTHERS. 2004. Southern Ocean Iron Enrichment Experiment: Carbon cycling in high- and low-Si waters. *Science* **16**: 408–414.
- COCHLAN, W. P. 2001. The heterotrophic bacterial response during a mesoscale iron enrichment experiment (IronEx II) in the eastern equatorial Pacific Ocean. *Limnol. Oceanogr.* **46**: 428–435.
- del Giorgio, P. A., and J. J. Cole. 2000. Bacterial energetics and growth efficiency, p. 289–325. *In* D. L. Kirchman [ed.], *Microbial ecology of the oceans*. Wiley-Liss.
- DUCKLOW, H. W. 2003. Seasonal production and bacterial utilization of DOC in the Ross Sea, Antarctica. *In* G. DiTullio and R. B. Dunbar [eds.], *Biogeochemistry of the Ross Sea*. *Ant. Res. Ser.* **78**: 143–158.
- , C. A. CARLSON, M. CHURCH, D. KIRCHMAN, D. SMITH, AND G. STEWARD. 2001a. The seasonal development of the bacterioplankton bloom in the Ross Sea, Antarctica, 1994–1997. *Deep-Sea Res. II* **48**: 4199–4221.
- , M.-L. DICKSON, D. L. KIRCHMAN, G. STEWARD, J. ORCHARDO, J. MARRA, AND F. AZAM. 2000. Constraining bacterial production, conversion efficiency and respiration in the Ross Sea, Antarctica, January–February, 1997. *Deep-Sea Res. II* **47**: 3227–3247.
- , D. L. KIRCHMAN, AND T. R. ANDERSON. 2002. The magnitude of spring bacterial production in the North Atlantic Ocean. *Limnol. Oceanogr.* **47**: 1684–1693.
- , J. L. OLIVER, AND W. O. SMITH, JR. 2003. The role of iron as a limiting nutrient for marine plankton processes, p. 295–310. *In* J. M. Melillo, C. B. Field, and B. Moldan [eds.], *Interactions of the major biogeochemical cycles (SCOPE 61): Global change and human impacts*. Island Press.
- , D. K. STEINBERG, AND K. O. BUESSELER. 2001b. Upper ocean carbon export and the biological pump. *Oceanography* **14**: 50–58.
- FUHRMAN, J. A., AND F. AZAM. 1982. Thymidine incorporation as a measure of heterotrophic bacterioplankton production in marine surface waters: Evaluation and field results. *Mar. Biol.* **66**: 109–120.
- FUKUDA, R., H. OGAWA, T. NAGATA, AND I. KOIKE. 1998. Direct determination of carbon and nitrogen contents of natural bacterial assemblages in marine environments. *Appl. Environ. Microbiol.* **64**: 3352–3358.
- GASOL, J. M., AND X. A. G. MORAN. 1999. Effects of filtration on bacterial activity and picoplankton community structure as assessed by flow cytometry. *Aquat. Microb. Ecol.* **16**: 251–264.
- GOLDMAN, J. C., AND M. R. DENNETT. 1991. Ammonium regeneration and carbon utilization by marine bacteria grown on mixed substrates. *Mar. Biol.* **109**: 369–378.
- HALL, J. A., AND K. SAFI. 2001. The impact of in situ Fe fertilisation on the microbial food web in the Southern Ocean. *Deep-Sea Res. II* **48**: 2591–2613.
- HISCOCK, M. R., AND OTHERS. 2003. Primary productivity and its regulation in the Pacific sector of the Southern Ocean. *Deep-Sea Res. II* **50**: 533–558.
- , G. R. DiTULLIO, AND K. W. BRULAND. 1993. Iron and regenerated production: Evidence for biological iron recycling in two marine environments. *Limnol. Oceanogr.* **38**: 1242–1255.
- HUTCHINS, D. A., A. E. WITTER, A. BUTLER, G. W. LUTHER III. 1999. Competition among marine phytoplankton for different chelated iron species. *Nature* **400**: 858–861.
- KIRCHMAN, D. L. 1990. Limitation of bacterial growth by dissolved organic matter in the subarctic Pacific. *Mar. Ecol. Progr. Ser.* **62**: 47–54.
- , B. MEON, M. T. COTTRELL, D. A. HUTCHINS, D. WEEKS, AND K. W. BRULAND. 2000. Carbon versus iron limitation of bacterial growth in the California upwelling regime. *Limnol. Oceanogr.* **45**: 1681–1688.
- LANDRY, M. R., AND OTHERS. 2000. Biological response to iron fertilization in the eastern equatorial Pacific (IronEx II). I. Microplankton community abundances and biomass. *Mar. Ecol. Progr. Ser.* **201**: 27–42.
- LEBARON, P., S. SERVAIS, H. AGOGUÉ, C. COURTIES, AND F. JOUX. 2001. Does the high nucleic acid content of individual bacterial cells allow us to discriminate between active cells and inactive cells in aquatic systems? *Appl. Environ. Microbiol.* **67**: 1775–1782.
- MARTIN, J. H., AND OTHERS. 1994. Testing the iron hypothesis in ecosystems of the Equatorial Pacific Ocean. *Nature* **371**: 23–29.
- NAGATA, T. 2000. Production mechanisms of dissolved organic matter, p. 121–152. *In* D. L. Kirchman [ed.], *Microbial ecology of the oceans*. Wiley-Liss.
- PAKULSKI, J. D., R. B. COFFIN, S. L. HOLDER, R. DOWNER, P. AAS, M. M. LYONS, AND J. H. WADE. 1996. Iron stimulation of Antarctic bacteria. *Nature* **383**: 133–134.
- RUE, E. L., AND K. W. BRULAND. 1997. The role of organic complexation on ambient iron chemistry in the equatorial Pacific Ocean and the response of a mesoscale iron addition experiment. *Limnol. Oceanogr.* **42**: 901–910.
- SIMON, M., AND F. AZAM. 1989. Protein content and protein synthesis rates of planktonic marine bacteria. *Mar. Ecol. Progr. Ser.* **51**: 201–213.
- SMITH, D. C., AND F. AZAM. 1992. A simple economical method for measuring bacterial production synthesis rates in seawater. *Mar. Microb. Food Webs* **6**: 107–114.
- TORTELL, P. D., M. T. MALDONADO, AND N. M. PRICE. 1996. The role of heterotrophic bacteria in iron-limited ocean ecosystems. *Nature* **383**: 330–332.
- , M. T. MALDONADO, J. GRANGER, AND N. M. PRICE. 1999. Marine bacteria and biogeochemical cycling of iron in the oceans. *FEMS Microbiol. Ecol.* **29**: 1–11.
- TROUSSELLIER, M., C. COURTIES, P. LEBARON, AND P. SERVAIS. 1999. Flow cytometric discrimination of bacterial populations in seawater based on SYTO 13 staining of nucleic acids. *FEMS Microbiol. Ecol.* **29**: 319–330.

Received: 17 December 2003

Amended: 21 May 21 2004

Accepted: 13 June 2004